



A simple and timesaving method for the mass-transfer assessment of solvents used in physical absorption

Pierre-François Biard, Aurélie Coudon, Annabelle Couvert, Sylvain Giraudet

► To cite this version:

Pierre-François Biard, Aurélie Coudon, Annabelle Couvert, Sylvain Giraudet. A simple and timesaving method for the mass-transfer assessment of solvents used in physical absorption. Chemical Engineering Journal, Elsevier, 2016, in press. <10.1016/j.cej.2016.01.046>. <hal-01263045>

HAL Id: hal-01263045

<https://hal-univ-rennes1.archives-ouvertes.fr/hal-01263045>

Submitted on 1 Feb 2016

HAL is a multi-disciplinary open access archive for the deposit and dissemination of scientific research documents, whether they are published or not. The documents may come from teaching and research institutions in France or abroad, or from public or private research centers.

L'archive ouverte pluridisciplinaire **HAL**, est destinée au dépôt et à la diffusion de documents scientifiques de niveau recherche, publiés ou non, émanant des établissements d'enseignement et de recherche français ou étrangers, des laboratoires publics ou privés.

A simple and timesaving method for the mass-transfer assessment of solvents used in physical absorption

Pierre-François BIARD^{a1}, Aurélie COUDON^a, Annabelle COUVERT^a, Sylvain GIRAUDET^a

^aÉcole Nationale Supérieure de Chimie de Rennes, CNRS, UMR 6226, 11 Allée de Beaulieu, CS 50837, 35708 Rennes Cedex 7, France

Abstract

A simple dynamic absorption procedure to assess the mass-transfer performances of a solvent toward a selected gaseous solute is presented. Absorption was operated semi-continuously at transient state until the equilibrium was reached without solvent recirculation. Four volatile organic compounds (VOC) more or less hydrophobic (toluene, acetone, dichloromethane, isopropanol) were absorbed in water and two heavy organic solvents (Bis(2-ethylhexyl) adipate DEHA and polydimethylsiloxane PDMS). A numerical resolution procedure was developed to simulate the gas-liquid mass-transfer and to deduce the VOC partition coefficients, expressed as the Henry's law constants, as well as the overall liquid-phase mass-transfer coefficients. The overall liquid-phase mass-transfer coefficients were correlated to the diffusion coefficients using the Higbie penetration theory. The results confirm the high selectivity of water whereas the two organic solvents, especially DEHA, exhibit rather good affinity with all VOC even if the Henry's law constants of the most soluble and the less soluble compounds for those solvents differ by 1 or 2 orders of magnitude. The liquid-film mass-transfer coefficients in the two organic solvents, even being more viscous, are larger than in water which confirms their good potential for hydrophobic VOC treatment.

Key words

Silicone oil; DEHA; absorption; Volatile Organic Compound; mass-transfer; partition coefficient

¹ Corresponding author : pierre-francois.biard@ensc-rennes.fr, +33 2 23 23 81 49

Highlights

- Heavy solvents (DEHA and PDMS) and water were assessed for the absorption of four VOC
- A simple and timesaving experimental procedure was developed
- Partition and mass-transfer coefficients were deduced from the experiments
- The two organic solvents tested, especially DEHA, exhibited rather good affinity with all VOC
- The liquid-film coefficient was 500% higher in PDMS and 30% higher in DEHA than in water

ACCEPTED MANUSCRIPT

1. Introduction

Combustion processes, road transport, waste and water treatments and many manufacturing industries generate gaseous emissions of volatile organic compounds (VOC) which are harmful for human health or environment [1]. Consequently, legislations in many developed countries become more and more drastic and impose to implement gas treatment processes to reduce VOC emissions.

Among the different gas treatment technologies, wet scrubbing is particularly attractive due to its simplicity and its high efficiency [2-5]. Gaseous pollutants are transferred in a liquid phase which can be either aqueous or organic. Aqueous scrubbing liquids are suitable for hydrophilic, acidic and/or basic compounds or when a fast reaction can be implemented such as for the H₂S absorption in a chlorine solution [6-8]. However for hydrophobic compounds, due to a poor solubility in water, absorption in aqueous solution is ineffective and organic solvents should be considered as an alternative. In that case, besides a good affinity with VOC, several constraints must be respected such as a low vapor tension, a low viscosity, a rather low cost, good chemical and thermal stabilities, a good chemical compatibility and a low toxicity [9, 10]. Since the last decade, a new generation of organic solvent, such as phthalates, polydimethylsiloxane (PDMS, a silicone oil), Bis(2-ethylhexyl) adipate (DEHA) or ionic liquids drew particular attention [11-16].

Besides the packing characteristics and some classic physico-chemical properties of the solvents such as its density, viscosity or surface tension, the mass-transfer rate in physical absorption mainly depends on two parameters related to the VOC/solvents interactions : (i) the gas-liquid partition coefficient (which accounts for the gas-liquid equilibrium) and (ii) the VOC diffusion coefficient (which accounts for the mass-transfer kinetics). The gas-liquid partition coefficients can be easily measured by static or dynamic methods [17-20]. Dynamic methods, whose the partition coefficient is deduced from the breakthrough curve, can be advantageously automated [17, 19, 20]. On the contrary, the diffusion coefficient determination requires sophisticated techniques and equipments to be measured, such as absorption in a laminar falling film contactor or thermogravimetric or

manometric methods [14, 21, 22]. Moreover, no universal and accurate correlation exists in the literature to quantify the diffusion coefficients in viscous solvents such as DEHA or PDMS [21]. Consequently, up to now, the assessment of organic solvents for VOC absorption is often based only on the VOC/solvent affinity evaluation through the gas-liquid partition coefficient measurement [18]. To screen and assess many solvents in a first stage, the liquid film mass-transfer coefficient of a solute in an investigated solvent determination and its comparison with a well-know solvent, such as water, is a pertinent strategy to confirm that the solute diffusion is not a limiting parameter [23]. This strategy would be even more valuable if the partition coefficient could be deduced simultaneously. Thus, the diffusion coefficient would be determined in a second stage with a more sophisticated technique.

This study presents a simple, reproducible and timesaving dynamic absorption procedure to assess the mass-transfer performances of a solvent toward a selected solute. This absorption was operated semi-continuously at transient state until the equilibrium was reached without solvent recirculation to simplify as much as possible the experimental procedure. Four more or less hydrophobic VOC, which belong to different chemical families currently involved in industrial emissions (toluene, acetone, dichloromethane, isopropanol) were absorbed in water and two heavy organic solvents (DEHA and PDMS). The VOC/solvent partition coefficients and overall liquid-phase mass-transfer coefficients were deduced from the breakthrough curves using a numerical procedure developed in this work. Then, the gas and liquid film mass-transfer coefficients were deduced and correlated to the gas and liquid diffusion coefficients using the Higbie penetration theory. The gas and liquid diffusion coefficients were calculated owing to Fuller et al. correlation and Hayduk-Laudie (water) or Wilke- Chang (DEHA, PDMS) correlations respectively.

2. Material and methods

2.1 Selection of volatile organic compounds and solvents

Table 1: Main physico-chemical properties of the selected VOC.

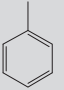
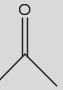
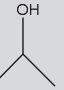
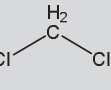
	Toluene	Acetone	Isopropanol	Dichloromethane
Formula				
Supplier	Acros Organics	Acros Organics	Acros Organics	Acros Organics
M (g mol⁻¹)	92.32	58.08	60.095	84.93
Purity (%)	99	99	99	99
ρ at 293K (kg m⁻³)	866.9	790	785	1326.6
10⁵D_G (m² s⁻¹)	0.74	1.04	1.01	1.02
10¹⁰D_{water} (m² s⁻¹)	7.96	10.2	9.88	11.3

Table 2: Main physico-chemical properties of the selected solvents. μ , σ and ρ are given at 293 K except for PDMS whose values are given at 298 K.


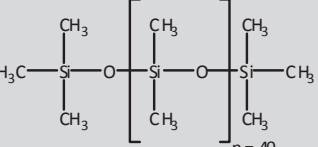
	Formula	M g mol ⁻¹	μ cP	ρ kg m ⁻³	σ mN m ⁻¹
Demineralized water	H ₂ O	18.0	1.0	1000	72.8
DEHA (Acros Organics)		370.58	12.5	922	31.0
PDMS (Bluestar Silicone)		3200	50.0	960	20.8

Table 1 and 2 respectively present the four VOC and the three solvents selected. The diffusion coefficients in the gas phase D_G (independent of the selected solvent) have been computed according to the Fuller et al. equation [8, 24]. The diffusion coefficients in water (D_{water}) have been computed with the Hayduk and Laudi correlation which is recommended for aqueous solutions [24]. The correlations usually used for the calculation of diffusion coefficients in organic solvents (Wilke-Chang, Scheibel, Tyn-Calus, Siddiqui-Lucas, etc.) were not developed for the case of a small solute (such as VOC) diffusing in a solvent composed of large molecules (such as DEHA and PDMS).

Therefore, they exhibit higher inaccuracy to predict diffusion coefficients in heavy solvents than in “traditional” organic or aqueous solvents [21, 22]. The VOC diffusion coefficients in each solvent calculated with these correlations are summarized in the Appendix 1 and compared to the few experimental data found in the literature (Tables A.1, A.2 and A.3). Except for the Wilke and Chang correlation, the molar volume of the solvents at their boiling point, which is unknown for DEHA and PDMS, were required. Therefore, for all these correlations, the DEHA and PDMS molar volumes were approximated at the ambient temperature instead of at the boiling temperature. The Tyn-Calus correlation undoubtedly overestimates the diffusion coefficients in DEHA and PDMS whereas the Hayduk-Minhas and Siddiqui-Lucas correlations seems to slightly underestimate them by comparison to the experimental values. The Scheibel and Wilke-Chang correlations appear more accurate providing values close to the experimental one. Nonetheless, the Scheibel correlation provides diffusion coefficients 40 to 75% higher for PDMS and 18 to 40% higher for DEHA than the Wilke-Chang correlation. For the case of phthalates, the Wilke and Chang correlation underestimates the experimental diffusion coefficient by 40-50% whereas the Scheibel equation overestimates it by 60-100% [21]. Therefore, the diffusion coefficients used in this paper were calculated with the Wilke-Chang correlation taking into account these observations and the fact that the unknown solvent molar volume at the boiling point is not required for this correlation. Nonetheless, the real diffusion coefficients might be slightly larger according to the Tables A.1 and 1.2. Nevertheless, the mass-transfer rate is usually rather poorly sensitive to the diffusion coefficient (which is reflected on the large discrepancy of the experimental data), *i.e.* a rather large inaccuracy on the diffusion coefficient calculation can be tolerated.

2.2 Experimental set-up and procedure

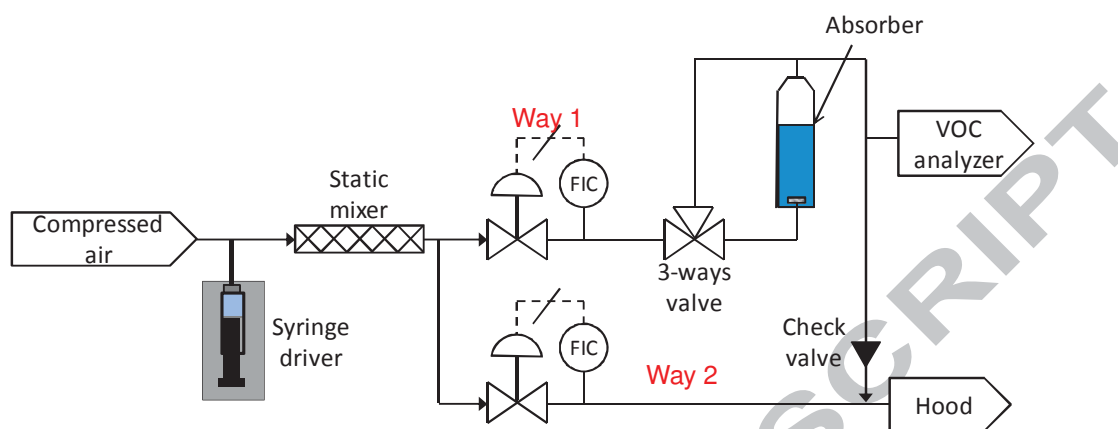


Figure 1: Flow and Process Diagram (FPD) of the experimental set-up.

The Flow and Process Diagram of the experimental set-up is presented in Fig. 1 (A picture of the experimental set-up is presented as supplementary material). The liquid VOC was vaporized in a compressed air flow to generate a synthetic vicious effluent. The amount of VOC vaporized was carefully controlled using a syringe-driver (KDS100, KdScientific) and a gas-tight syringe (SGE) to target an inlet VOC concentration around $80\text{--}85\text{ mg m}^{-3}$ (20-25 ppmv). The VOC/air mixture was homogenized by a static mixer, placed after the syringe needle.

The total air flow-rate ($1\text{ m}^3\text{ h}^{-1}$ at the Standard Temperature and Pressure (STP) = 1 bar and 273.15K according to the IUPAC) was controlled by means of two mass flow controllers in parallel (Bronkhorst). The first way was used to feed the gas-liquid contactor ($0.1\text{ m}^3\text{ h}^{-1}$ at STP) whereas the second way was directly drained ($0.9\text{ m}^3\text{ h}^{-1}$ at STP). These two ways were necessary to provide a sufficient total air flow-rate to vaporize VOC after the syringe driver. The glass gas-liquid contactor (6.4 cm of internal diameter, useful height of 16.0 cm), was fed by the bottom through a porous sparger to disperse the air flow in thin bubbles. The gas-liquid contactor was placed in a thermostatic bath to control the temperature at 293K ($\pm 1\text{ K}$). The gas-liquid contactor can be by-passed to analyze the inlet VOC concentration (a picture of the gas-liquid contactor is presented as supplementary material).

The gas-liquid contactor and the syringe were filled respectively by 100 mL of solvent (height of solvent = 3.1 cm without considering the gas hold-up which depended on the solvent) and 10 mL of VOC. The system was flushed using a total gas flow rate of $1 \text{ m}^3 \text{ h}^{-1}$ at STP (0.1 in the way 1, 0.9 in the way 2) by by-passing the gas-liquid contactor. The cleanliness of the system was checked by blank analysis. The syringe was held in the syringe-driver and the desired injection flow-rate was set. The inlet concentration was analyzed several times to control the stability of the VOC vaporization. At $t=0$, the 3-ways valve was switched to feed the gas-liquid contactor and the outlet concentration analysis was immediately started. The VOC concentration at the contactor outlet was sampled every 3.5 min and analyzed by a gas chromatograph (Agilent 6890N) equipped with a Flame Ionization Detector (FID) and a sampling injection loop to obtain the corresponding breakthrough curve. The sampling loop was composed of a six-port switching valve and a pump to feed the gas chromatograph with its content. The gas chromatograph calibration was directly achieved in dynamic conditions using the set-up at given gas and syringe driver flow-rates. When the equilibrium was reached, the VOC vaporization was stopped while keeping the contactor fed by compressed air to strip the absorbed VOC until the outlet concentration was negligible. Since the human intervention is restricted and that the flow control, VOC injection and VOC analysis are fully automated, this method is particularly reproducible and timesaving. Moreover, the potential systematic error risk is limited since the VOC quantification was checked for each experiment by comparing the gas concentration obtained at the plateau to the programmed inlet concentration.

3. Mass-transfer modeling

3.1 Problem positioning

The gas-liquid contactor was operated semi-continuously. The following characteristics and assumptions were considered:

- The liquid is perfectly mixed due to the gas bubbling which creates an intense stirring. This assumption has been controlled via the brief injection of a dye (indigo carmine) within the reactor and the fast homogenization of the solution.
- The gas phase follows a plug flow. Indeed, in such kind of gas-liquid contactor, the gas backmixing is almost negligible [25].
- The process is isothermal and achieved at 293 ± 1 K and atmospheric pressure. Indeed, absorption is an endothermic process but considering the low concentrations of VOC treated, it can be neglected.
- The gas flow rate (F_G) is constant between the inlet and the outlet of the contactor since the inlet VOC concentration is around only 20-25 ppm by volume.
- No chemical reaction happens in the liquid phase. The treated VOC are all neutrals so proton-transfer reactions (acid-base reactions) are unexpected using water.
- A 1D model (t, z) is relevant assuming that there is no radial concentration gradient in both phases.

The boundary and initial conditions are:

- C_G at the inlet (bottom) = $C_{G,i}$ = constant
- C_L at $t_0 = C_{L,0} = 0$
- $z = 0$ at the bottom and $Z = 3.1$ cm at the top of the liquid phase without gas bubbling.

The variables are:

- C_G at the outlet (top) = $C_{G,o} = f(t)$
- C_L at any time = C_L^t

3.2 Mass balance

The mass balance can be written:

$$\text{Gas inlet} = \text{Gas outlet} + \text{transfer} \Rightarrow F_G C_{G,i} = F_G C_{G,o} + V \frac{dC_L}{dt} \quad \text{Eq. 1.}$$

$$\Rightarrow F_G (C_{G,i} - C_{G,o}) = V \frac{dC_L}{dt} \quad \text{Eq. 2.}$$

This equation can be integrated over time proceeding by discretization considering a small time interval Δt :

$$F_G (C_{G,i} - \bar{C}_{G,o}) = \frac{V}{\Delta t} (C_L^{t+\Delta t} - C_L^t) \quad \text{Eq. 3.}$$

With $\bar{C}_{G,o}$ the average VOC gas concentration at the outlet measured during Δt :

$$\bar{C}_{G,o} = \frac{C_{G,o}^{t+\Delta t} + C_{G,o}^t}{2} \quad \text{Eq. 4.}$$

It leads to:

$$C_L^{t+\Delta t} = C_L^t + F_G \frac{\Delta t}{V} (C_{G,i} - \bar{C}_{G,o}) \quad \text{Eq. 5.}$$

The liquid concentration over time can be calculated through Eq. 6:

$$C_L^t = \frac{F_G}{V} \sum_{j=1}^n \Delta t \left(C_{G,i} - \frac{C_{G,o}^{t+\Delta t} + C_{G,o}^t}{2} \right) \text{ with } j \text{ the number of time interval} \quad \text{Eq. 6.}$$

3.3 Mass-transfer rate equation

The mass-transfer rate (dJ) per section (S) of gas-liquid contactor ($\text{mol s}^{-1} \text{m}^{-2}$) is calculated through

Eq. 7:

$$\frac{dJ}{S} = F_G \frac{dC_G}{S} = K_L a^\circ (C_L^{eq} - C_L) dz \quad \text{Eq. 7.}$$

K_L is the overall liquid-side mass-transfer coefficient (m s^{-1}). a° is the interfacial area relative to the liquid volume V ($\text{m}^2 \text{m}^{-3}$). C_L^{eq} is the liquid concentration (mol m^{-3}) at the gas-liquid interface at the equilibrium with the gas concentration. It can be easily calculated for dilute solutions using the Henry's law (Eq. 8):

$$C_L^{eq} = \frac{C_G}{H_d} \quad \text{Eq. 8.}$$

H_d is the dimensionless Henry's law constant ($\text{mol Nm}^{-3}/\text{mol m}^{-3}$) of the treated VOC in the selected solvent (partition coefficient). It leads to:

$$\Rightarrow F_G dC_G = K_L a^\circ \left(\frac{C_G}{H_d} - C_L \right) S dz \quad \text{Eq. 9.}$$

After integration during a time-interval Δt :

$$\Rightarrow F_G \int_{C_{G,i}}^{\bar{C}_{G,o}} dC_G = K_L a^\circ \int_0^Z \left(\frac{C_G}{H_d} - C_L \right) S dz \quad \text{Eq. 10.}$$

The left-hand term can be easily integrated whereas the right-hand term must be solved using a variable modification. The solution is well-known and can be found in many book dealing with gas-liquid mass-transfer [8]. It involves the logarithmic average concentration assuming a gas plug flow and a perfectly mixed liquid phase:

$$\Rightarrow F_G(C_{G,i} - \bar{C}_{G,o}) = K_L a^\circ V \frac{\left(\frac{C_{G,i}}{H_d} - \bar{C}_L\right) - \left(\frac{\bar{C}_{G,o}}{H_d} - \bar{C}_L\right)}{\frac{C_{G,i}}{H_d} - \bar{C}_L} \quad \text{Eq. 11.}$$

$$\ln \frac{\frac{C_{G,o}}{H_d} - \bar{C}_L}{\frac{C_{G,i}}{H_d} - \bar{C}_L}$$

\bar{C}_L is the average liquid concentration during a time-interval Δt :

$$\bar{C}_L = \frac{C_L^{t+\Delta t} + C_L^t}{2} \Leftrightarrow C_L^{t+\Delta t} = 2\bar{C}_L - C_L^t \quad \text{Eq. 12.}$$

After mathematical treatment (presented in details in Appendix 2), the liquid and outlet gas concentrations at $t + \Delta t$ are calculated through respectively Eqs 13 and 14:

$$C_L^{t+\Delta t} = 2 \frac{\frac{C_{G,i}}{H_d} (1 - \exp(B)) - 2AC_L^j \exp(B)}{1 - \exp(B)(1 + 2A)} - C_L^j \quad \text{Eq. 13.}$$

$$\text{With } A = \frac{V}{H_d F_G \Delta t} \text{ and } B = AK_L a^\circ \Delta t = \frac{K_L a^\circ V}{H_d F_G}$$

$$C_{G,o}^{t+\Delta t} = 2\bar{C}_{G,o} - C_{G,o}^t = 2 \left(C_{G,i} - \frac{V}{F_G \Delta t} (C_L^{t+\Delta t} - C_L^t) \right) - C_{G,o}^t \quad \text{Eq. 14.}$$

To initialize the resolution, $C_{G,o}$ at $t=0$ must be calculated. The time necessary for the first bubbles to reach the top of the reactor is neglected compared to the experiment duration. In this case, Eq. 11 can be rewritten considering that $C_L = 0$:

$$\Rightarrow F_G(C_{G,i} - C_{G,o}^{t=0}) = \frac{K_L a^\circ V}{H_d} \frac{(C_{G,i} - C_{G,o}^{t=0})}{\ln \frac{C_{G,i}}{C_{G,o}^{t=0}}} \quad \text{Eq. 15.}$$

$$\Rightarrow C_{G,o}^{t=0} = C_{G,i} \exp\left(-\frac{K_L a^\circ V}{F_G H_d}\right) \quad \text{Eq. 16.}$$

Except H_d and $K_L a^\circ$, all the parameters are known and controlled.

3.4 Henry's law constant determination

H_d can be deduced from the liquid concentration at the plateau of the breakthrough curve corresponding to the gas-liquid equilibrium and to a zero removal efficiency ($C_{G,o} = C_{G,i}$):

$$H_d = \frac{C_{G,i} (\text{mol Nm}^{-3})}{C_{L,saturation} (\text{mol m}^{-3})} \quad \text{Eq. 17.}$$

Nm^{-3} refers to the Standard Temperature and Pressure. The liquid concentration was unmeasured but calculated using the mass-balance (Eq. 6) assuming a negligible solute adsorption on the glass wall. H_d can be converted to the Henry's law constant in $\text{Pa m}^3 \text{mol}^{-1}$ by a multiplication by the ideal gas constant R and the standard temperature (273.15 K).

3.5 $K_L a^\circ$ determination

$K_L a^\circ$ characterizes the mass-transfer kinetics of any VOC in a solvent through hydrodynamic and mass-transfer performances considerations. This value depends on the gas flow-rate which was kept constant. With identical operating conditions for every experiment, a° is expected to be constant for a given solvent whereas K_L could be correlated to the diffusion coefficients in the liquid and the gas phases.

$K_L a^\circ$ was determined for each VOC/solvent couple by numerical resolution using the procedure presented in Fig. 2 and the Excel® solver. This procedure is build on iterative calculations according to Eqs. 13 and 14. The Error Function (EF) minimized to determine $K_L a^\circ$ was based on the least-square methodology:

$$\Rightarrow EF = \sum_{j=1}^n \left(\frac{(C_{G,o}^{t+\Delta t})_{\text{exp}} - (C_{G,o}^{t+\Delta t})_{\text{model}}}{(C_{G,o}^{t+\Delta t})_{\text{exp}}} \right)^2 \quad \text{Eq. 18.}$$

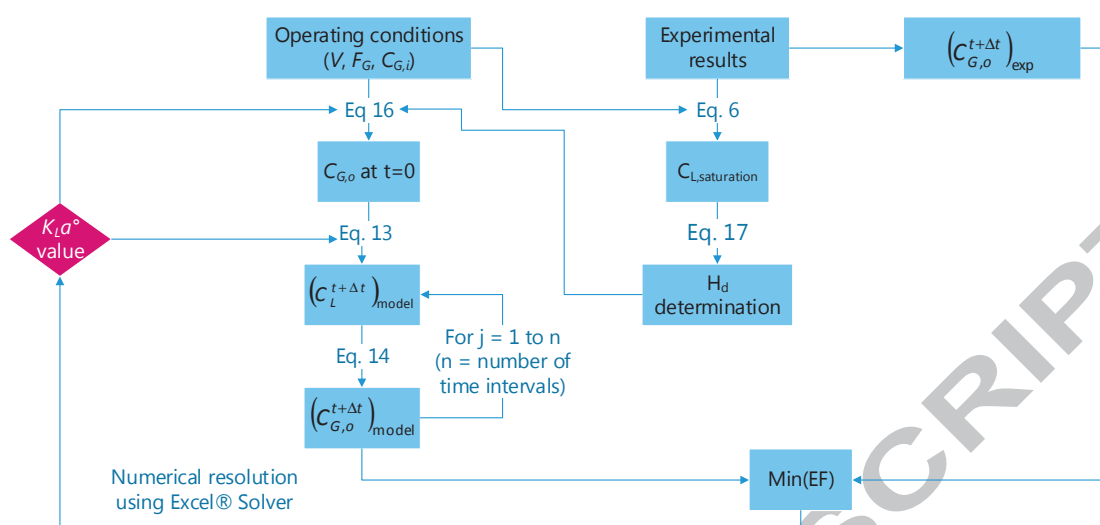


Figure 2: Numerical resolution procedure applied for the $K_L a^\circ$ determination.

4. Results and discussion

4.1 Theoretical and mathematical background

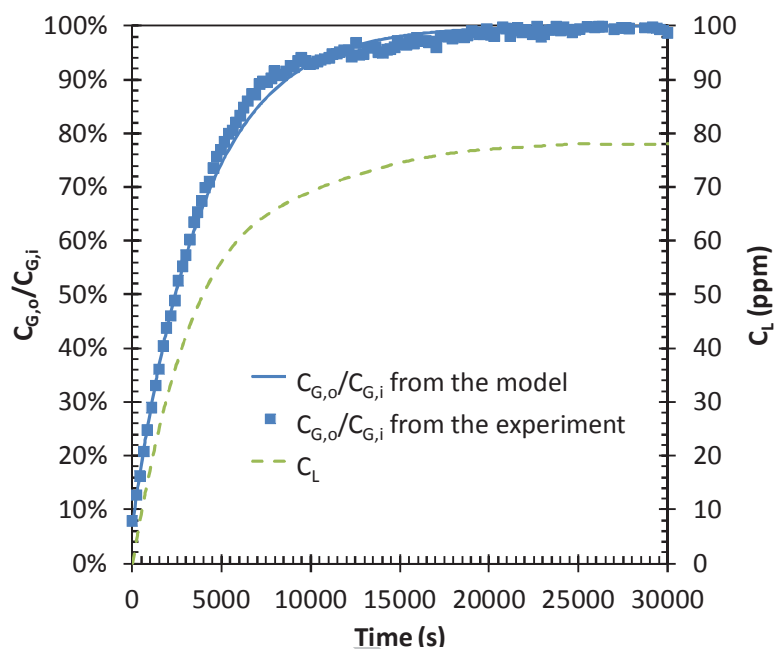


Figure 3: Example of a breakthrough curve (acetone removal in water). The other curves are accessible as supplementary material.

Table 3: Henry's law constant (H_d in $(\text{mol Nm}^{-3})/(\text{mol m}^{-3})$ and H in $\text{Pa m}^3 \text{mol}^{-1}$) determined through the dynamic absorption experiments. t_{eq} is the time necessary to reach the equilibrium.

Solvent	Water			DEHA			PDMS			
	VOC	t_{eq} (s)	H_d	H	t_{eq} (s)	H_d	H	t_{eq} (s)	H_d	H
Toluene		Fast	Undetermined	35000	$3.35 \cdot 10^{-4}$	0.76	21000	$5.99 \cdot 10^{-4}$	1.36	
Dichloromethane		Fast	Undetermined	9200	$2.08 \cdot 10^{-3}$	4.73	2500	$9.70 \cdot 10^{-3}$	22.01	
Isopropanol		$>10^5$	$1.37 \cdot 10^{-4}$	0.31	5000	$2.89 \cdot 10^{-3}$	6.57	3500	$9.44 \cdot 10^{-3}$	21.42
Acetone		30000	$1.00 \cdot 10^{-3}$	2.28	6500	$5.59 \cdot 10^{-3}$	12.68	1000	$2.33 \cdot 10^{-2}$	52.97

During a typical experiment, due to the VOC accumulation in the liquid phase (green dash line deduced from Eq. 6), the outlet gas concentration (blue points and straight line) increases gradually to the inlet gas concentration until a plateau corresponding to the gas-liquid equilibrium is reached

(Fig. 3). The initial removal efficiency is non zero even if the solvent is unloaded with VOC (Eq. 16). The saturation times (t_{eq}) necessary to reach the plateau range from 10^3 to 35×10^3 s (Table 3). Even if the mass-transfer rate increases with the affinity (see 4.2), t_{eq} increases which seems paradoxical but which is justified by a higher absorption capacity. For the dichloromethane and toluene absorption in water, due to a low affinity with water, the removal efficiencies were too low to be accurately measured.

The Henry's law constants (H_d and H according to § 3.4) are calculated taking into account the gas and liquid concentrations at the plateau (Table 3) and compared to the values found in the literature (Table 4). The agreement between the experimental values and the literature values is good for DEHA and water, taking into account that H_d is rather sensitive to the temperature. It can justify why the measured values are always lower than the values of the literature determined at 298 K. Since the silicone oils are not standard products and may contain different amount of impurities and moisture even for different batches of the same commercial product, the toluene Henry's law constants values determined in several studies are dispersed from 1.7 to $12.1 \text{ Pa m}^3 \text{ mol}^{-1}$ (Table 4). Moreover, the Henry's law constants are often provided in the literature under their dimensionless form (mol m^{-3} of gas / mol m^{-3} of liquid) whose the temperature and pressure taken to express the gas volume are often not specified providing an additional inaccuracy when converting them in $\text{Pa m}^3 \text{ mol}^{-1}$. Therefore, the relative errors have not been calculated for the toluene/PDMS couple in the Table 4. It is noteworthy that the evolution of H with the viscosity does not follow any logic. **Guillerm et al. (2015) concluded that there was no significant influence of the PDMS viscosities (between 5 and 105 mPa s) on the toluene partition coefficient.** The experimental value measured in this study is close to the value found by Heymes et al. in 2006.

Table 4: Comparison between some experimental Henry's law constant values (in $\text{Pa m}^3 \text{mol}^{-1}$) and the values of the literature. RE is the relative error.

Solvent	VOC	H exp (293 K)	H literature	RE
Water	Toluene	ND	510 at 293 K [26]	
Water	Dichloromethane	ND	220 at 293 K [26]	
Water	Acetone	2.28	2.61 at 298 K [27]	12.6%
Water	Acetone	2.28	2.68 at 298 K [26]	14.9%
Water	Propanol	0.31	0.31 at 298 K [28]	
DEHA	Toluene	0.76	0.88 at 298 K [29]	15.8%
DEHA	Toluene	0.76	0.79 at 298 K [13]	3.7%
DEHA	Dichloromethane	22.01	17.85 at 298 K (unpublished result)	23.3%
PDMS	Toluene	1.36	2.9 at 298 K [18] (PDMS @ 50 cP)	Irrelevant
PDMS	Toluene		6.9 at 298 K [30] (PDMS @ 50 cP)	Irrelevant
PDMS	Toluene		12.1 at 298 K [31] (PDMS @ 100 cP)	Irrelevant
PDMS	Toluene		2.7 at 298 K [18] (PDMS @ 100 cP)	Irrelevant
PDMS	Toluene		3.1 at 298 K [18] (PDMS @ 20 cP)	Irrelevant
PDMS	Toluene		1.7 at 298 K [13] (PDMS @ 20 cP)	Irrelevant
PDMS	Toluene		2.7 at 298 K [18] (PDMS @ 5 cP)	Irrelevant
PDMS	Toluene		2.3 at 298 K [32] (PDMS @ 5 cP)	Irrelevant

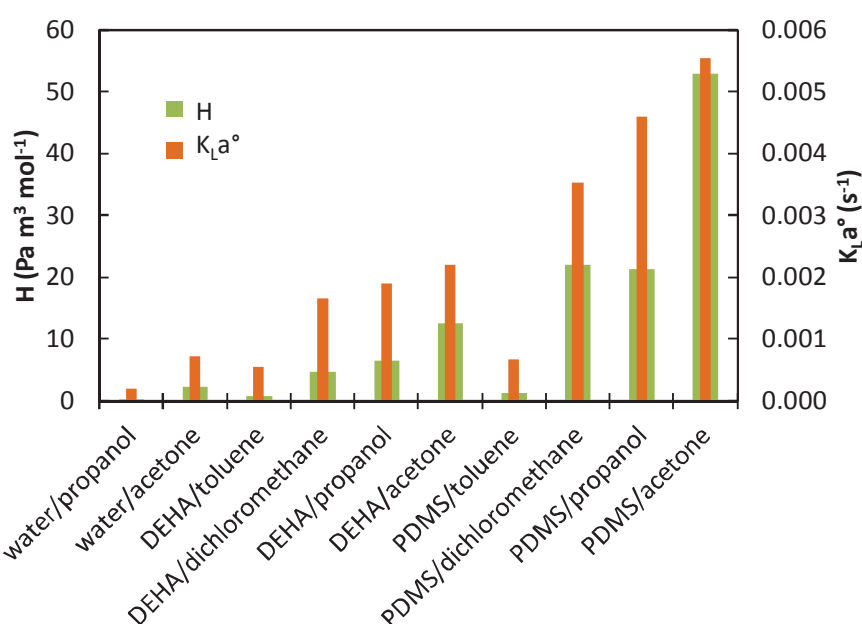


Figure 4: Synthesis of the H and $K_L a^\circ$ values for the different VOC/solvent couples.

The two organic solvents, and especially DEHA, exhibit good affinity with all VOC, whereas the results highlight the selective character of water. Nonetheless, two VOC among the four studied (propanol

and acetone) have a better affinity towards water than the organic solvents. This is justified by the good polarity of both VOC. The four VOC have a better affinity towards DEHA than PDMS. In regards of its lower viscosity, DEHA seems to be a more promising solvent than PMDS whose affinity with the selected VOC is rather disappointing. However, since DEHA is biodegradable, only physical regeneration methods can be considered (distillation, pervaporation, stripping, membrane separation, etc.) whereas PDMS can be recycled by a low-cost biological step [9, 33].

4.2 $K_L a^\circ$ determination – Mass-transfer kinetics assessment

The Henry's law constant values account for the gas-liquid equilibrium. The mass-transfer rate, *i.e.* the absorption kinetics, depends directly on the overall liquid-side mass-transfer coefficient ($K_L a^\circ$). The $K_L a^\circ$ values were determined following the numerical procedure summarized in Fig 2. They are as expected in the range 10^{-4} - 10^{-3} s⁻¹ (Table 5 and Fig. 4) and consistent with the values reported in the literature for similar experiments and VOC/solvent couples [12, 29]. The goodness of fit is confirmed by the agreement between the experimental data and the model represented by the straight lines and by the determination coefficients (Table 5) between the outlet concentrations measured experimentally and those obtained from the model (Eq. 14). It also emphasizes that the discretization path used for the numerical resolution was sufficient (equal to the sampling time = 3.5 min). A discretization path lower than 5% of the equilibrium time is recommended. This $K_L a^\circ$ determination method is particularly more efficient and accurate than the method based on a linear regression since the error propagation is limited [13, 29]. For example, considering acetone removal in water, the $K_L a^\circ$ value determined by the linear regression method was underestimated by 25% and the determination coefficient of the linear regression was only 0.82.

The $K_L a^\circ$ value increases when the Henry's law constant increases (*i.e.* when the solvent/VOC affinity decreases) for any couple solvent/VOC. The reliability of this result, which was expected, but which could seem paradoxical at first glance, will be confirmed in the next section (4.3). Nonetheless, since the mass-transfer rate (J) is the product of $K_L a^\circ$ and the concentration gradient (Eq. 7), the mass-

transfer rate, which has been calculated at the initial time (Table 5), remains significantly higher for the compounds with a high affinity for the solvent mainly due to a poorer mass-transfer resistance in the liquid side, the resistance in the gas phase being almost identical for all compounds since their diffusion coefficients are close.

ACCEPTED MANUSCRIPT

4.3 $K_L a^\circ$ modeling

The reliability of the $K_L a^\circ$ values determined should be assessed taking into account the diffusion in both phases. The overall volumetric liquid-side mass-transfer coefficient $K_L a^\circ$ depends on the local one ($k_L a^\circ$ and $k_G a^\circ$) through Eq. 19:

$$\frac{1}{K_L a^\circ} = \frac{1}{k_L a^\circ} + \frac{RT}{H k_G a^\circ} \quad \text{Eq. 19.}$$

According to the Higbie penetration theory [34], the gas-liquid interface consists of a variety of small liquid and gas elements, which are continuously brought up to the surface from the bulk by the motion of phases themselves. The local mass-transfer coefficients are directly proportional to the square root of the diffusion coefficients of the solute in both phases (D_L and D_G in $\text{m}^2 \text{s}^{-1}$, compiled in Tables 1, A.1 and A.2) and inversely proportional to the square root of the ages τ_G and τ_L of the element as follows:

$$k_L a^\circ = \sqrt{\frac{4D_L}{\pi\tau_L}} a^\circ \quad \text{Eq. 20.}$$

$$k_G a^\circ = \sqrt{\frac{4D_G}{\pi\tau_G}} a^\circ \quad \text{Eq. 21.}$$

Then:

$$\frac{1}{K_L a^\circ} = \frac{1}{\sqrt{\frac{4D_L}{\pi\tau_L}} a^\circ} + \frac{RT}{H \sqrt{\frac{4D_G}{\pi\tau_G}} a^\circ} \quad \text{Eq. 22.}$$

Eq. 22 can be rewritten to lead to the following linear relationship:

$$\frac{\sqrt{\frac{4D_L}{\pi}}}{K_L a^\circ} = \frac{\sqrt{\tau_L}}{a^\circ} + \frac{\sqrt{\tau_G}}{a^\circ} \frac{RT}{H} \sqrt{\frac{D_L}{D_G}} \quad \text{Eq. 23.}$$

It should be stressed that the correlations used for the liquid diffusion calculation can present a rather high uncertainty (section 2.1). In the case of the gas diffusion coefficients, the diffusion coefficients vary only with the nature of the compounds since the gas phase was identical (air). Fig. 5

represents $\left(\frac{\sqrt{\frac{4D_L}{\pi}}}{K_L a^\circ}\right) = f\left(\frac{RT}{H} \sqrt{\frac{D_L}{D_G}}\right)$ for the three solvents and confirms the linear relationship for

DEHA and PDMS. The values of $\frac{\sqrt{\tau_L}}{a^\circ}$ and $\frac{\sqrt{\tau_G}}{a^\circ}$ can be simply determined respectively with the y-

intercept and the slope (Table 7). The orders of magnitude for the different solvents are close, which seems to confirm the reliability of the experimental values of $K_L a^\circ$ determined. From these values of

$\frac{\sqrt{\tau_L}}{a^\circ}$ and $\frac{\sqrt{\tau_G}}{a^\circ}$, theoretical values of $K_L a^\circ$, in good agreement with the experimental one, have been

calculated (Table 6).

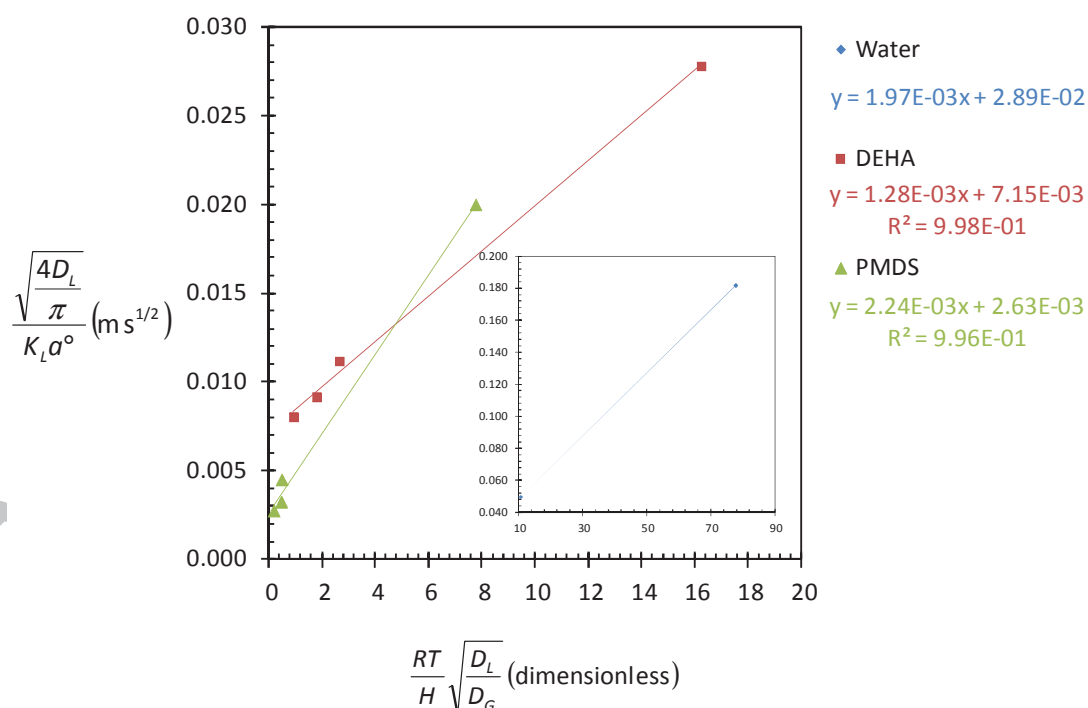


Figure 5: Application of the graphical method according to Eq. 23.

Table 7: Values of $\frac{\sqrt{\tau_L}}{a^\circ}$ and $\frac{\sqrt{\tau_G}}{a^\circ}$ (in $\text{m s}^{1/2}$) determined by both methods. The relative average

error (RAE) is calculated between the experimental values of $K_L a^\circ$ and those deduced from Eq. 23.

To achieve a sensitivity analysis to D_L , two rather pessimistic scenario assuming that D_L in DEHA and PDMS (Tables A.1 and A.2) have been under and overestimated by a factor 2 are considered.

	D_L				$D_L/2$		$D_L \times 2$	
Solvent	$10^3 \times \frac{\sqrt{\tau_L}}{a^\circ}$	$10^3 \times \frac{\sqrt{\tau_G}}{a^\circ}$	RAE	$\frac{\tau_L}{\tau_G}$	$10^3 \times \frac{\sqrt{\tau_L}}{a^\circ}$	$\frac{\tau_L}{\tau_G}$	$10^3 \times \frac{\sqrt{\tau_L}}{a^\circ}$	$\frac{\tau_L}{\tau_G}$
Water	28.9	1.97		215	Not relevant			
DEHA	7.15	1.28	3.3%	31.2	5.05	15.6	10.1	62.3
PDMS	2.63	2.24	11.0%	1.4	1.86	0.69	3.72	2.8

According to Eq. 23, the linear regression is sensitive to D_L , D_G , $K_L a^\circ$ and H . D_L in water and D_G are estimated with a satisfactory accuracy (Table 1). $K_L a^\circ$ and H were measured and suffer from random errors, which should influence the goodness of fit but not significantly the y-intercept and the slope of the linear regression. However, D_L in DEHA and PDMS are calculated with a high uncertainty owing to their high viscosities and molar volumes. The sensitivity of the linear regression to this parameter should be therefore evaluated. In this case, D_L suffers from significant systematic errors which should lead to real values of D_L under or overestimated by a more or less constant factor for each solvent. As rather pessimistic scenarios, a constant factor of 2 has been considered for the sensitivity analysis. Only the y-intercept ($\sqrt{\tau_L}/a^\circ$) is affected and its variation remains limited to the square root of the considered factor (Table 7).

4.4 Discussion

With the values of $\frac{\sqrt{\tau_L}}{a^\circ}$ and $\frac{\sqrt{\tau_G}}{a^\circ}$, it was possible to evaluate the local volumetric mass-transfer coefficients in both phases ($k_L a^\circ$ and $k_G a^\circ$) through Eqs. 20 and 21 and control their reliability. The values are consistent with the orders of magnitude encountered in the literature (Table 6) [8]. Since a variation of the gas film mass-transfer coefficient k_G is unexpected for a given VOC whatever the

considered solvents, the interfacial area ratios between the different solvents can be evaluated (Table 8). DEHA appears to be the solvent which exhibits the highest interfacial area. This was confirmed by visual observations which emphasized a high liquid expansion (*i.e.* high gas retention) combined to smaller gas bubbles using the DEHA. Its low interfacial tension and moderate viscosity can justify this result ($\sigma = 31 \text{ mN m}^{-1}$ at 298 K compared to 72 mN m^{-1} for water). Then, the ratios between the liquid-film mass-transfer coefficients (k_L) of the different solvents could be evaluated. The results are quite surprising since the two organic solvents, and especially PDMS, exhibit the highest values even if their diffusion coefficients (Table 1) are significantly lower (especially due to larger viscosities). It conveys a shorter renewal time for the organic solvents which favors the mass-transfer. In compensation, a higher energy loss would be expected to justify these results. Unfortunately, the pressure drops were unmeasured. Indeed, the ratio $\frac{\tau_L}{\tau_G}$ can be easily determined for each solvent (Table 7). Since τ_G is not expected to vary for the different solvents, τ_L should be 6.9 times and 157 times higher in water than in respectively DEHA and PDMS. It justifies why the mass-transfer performances are not significantly altered by the larger viscosity of DEHA and PDMS. The lower surface tension of DEHA and PDMS can be evoked as a possible reason of this observation. More data with other solvents would be necessary to justify it. Consequently, even if the diffusion of organic compounds in organic solvents is hindered compared to water, the mass-transfer properties remain fully acceptable confirming the high absorption potential of these solvents. This has been confirmed for toluene absorption in DEHA and PDMS using packed columns [35, 36]. Nonetheless, these comparisons between the organic solvents and water must be considered carefully since only two points were obtained with water.

Table 8: Values of the interfacial areas and liquid-side mass-transfer coefficients ratios.

$a^{\circ}_{\text{DEHA}}/a^{\circ}_{\text{water}}$	$a^{\circ}_{\text{DEHA}}/a^{\circ}_{\text{PDMS}}$	$a^{\circ}_{\text{water}}/a^{\circ}_{\text{PDMS}}$	$k_{L,\text{DEHA}}/k_{L,\text{water}}$	$k_{L,\text{DEHA}}/k_{L,\text{PDMS}}$	$k_{L,\text{water}}/k_{L,\text{PDMS}}$
1.54	1.75	1.14	1.28	0.25	0.19

Finally, the percentage of resistance in the liquid phase (R_L), which is a pertinent parameter to assess in which phase the mass-transfer is mainly limited, has been evaluated [37, 38]:

$$R_L = \left(1 + \frac{k_L a^\circ}{H_d k_G a^\circ} \right)^{-1} \quad \text{Eq. 24.}$$

Except in a few cases, no resistance in any phase should be neglected even if that is often considered in the literature (Table 6) [36]. It also justifies why, even if the uncertainty of the calculated liquid diffusion coefficients is quite large, their influence for the $K_L a^\circ$ determination remains limited. Indeed, since a non negligible part of the resistance is located in the gas phase, this effect is smoothed.

From the tools developed above, it would be possible to simulate the dynamic absorption of any VOC in the three selected solvents provided that the Henry's law constant and the liquid diffusion coefficient are known. From such simulation, it appears that this technique can be hardly applied for compounds/solvent couples characterized by a Henry's law constant higher than around $100 \text{ Pa m}^3 \text{ mol}^{-1}$ to be able to accurately measure the outlet gas concentration, except if the liquid volume increases and/or the gas flow rate decreases.

5. Conclusion and perspectives

A simple dynamic absorption procedure to assess the mass-transfer performances of a solvent toward a selected gaseous solute is presented. Dynamic absorption of four VOC (dichloromethane, propanol, toluene and acetone) was carried out batch wise in three solvents (water, DEHA and PDMS). DEHA and PDMS are promising heavy solvents for gas-liquid operations due to a negligible volatility. A numerical resolution procedure was developed to simulate the gas-liquid mass-transfer and to deduce the VOC partition coefficients, expressed as the Henry's law constants, as well as the overall liquid-phase mass-transfer coefficients. Contrarily to water, the two organic solvents, especially DEHA, exhibit rather good affinity with all VOC (Henry's law constants from 0.76 to 12.68 Pa m³ mol⁻¹ for DEHA and from 1.36 to 52.97 Pa m³ mol⁻¹ for PDMS). The most hydrophobic compounds (toluene and dichloromethane) have the best affinity toward DEHA and PDMS. Therefore, the combination of two absorption steps in series working with water and a heavy organic solvent can be a feasible option to treat complex gas effluent. The evaluation of the liquid-film mass-transfer coefficients (k_L) highlights good mass-transfer performances of DEHA and PDMS. Indeed, k_L is 10% larger in DEHA and 500% larger in PDMS than in water, which demonstrates that mass-transfer in viscous solvents is effective. The knowledge of the VOC Henry's law constant in each solvents will enable to simulate the VOC absorption in packed column and to confirm the potential of these solvents.

6. Funding source

The research leading to these results has received funding from the European Union's Seventh Framework Program (FP7/2007-2013) managed by REA-Research Executive Agency (<http://ec.europa.eu/research/rea>) under grant agreement n° 315250 (CARVOC program).

7. Acknowledgment

We thank Angela Alvarez and Manuel Román from Contactica (Spain) for the management of the project.

ACCEPTED MANUSCRIPT

Glossary

a° : interfacial area (relative to the liquid volume) ($\text{m}^2 \text{m}^{-3}$)

C_G : VOC gas concentration (mol Nm^{-3})

C_L : VOC liquid concentration (mol m^{-3})

D_G (D_L): diffusion coefficient at infinite dilution of a solute in the gas phase (liquid phase)

Eff: removal efficiency

EF: error function

F: flow rate ($\text{m}^3 \text{s}^{-1}$ or L s^{-1} , often expressed in the normal conditions of temperature and pressure)

H: Henry's law constant ($\text{Pa m}^3 \text{mol}^{-1}$)

H_d : dimensionless Henry's law constant ($(\text{mol Nm}^{-3})/(\text{mol m}^{-3})$)

j : number of time intervals

k_G : gas-film mass-transfer coefficient (m s^{-1})

k_L : liquid-film mass-transfer coefficient (m s^{-1})

$K_L a^\circ$: overall volumetric liquid-side mass-transfer coefficient (s^{-1})

P: absolute pressure in the reactor (Pa)

Pa: parachor ($\text{g}^{1/4} \text{cm}^3 \text{mol}^{-1} \text{s}^{-1/2}$)

RE: relative error between a theoretical and an experimental value (%)

RAE: relative average error between a set of experimental and theoretical values (%)

R_L : relative mass-transfer resistance in the liquid phase (%)

S: contactor section (m^2)

t: time (s)

t_{eq} : time necessary to reach the equilibrium (s)

S_{col} : column section (m^2)

T: temperature of the reactor ($^\circ\text{C}$ or K)

T_b : boiling temperature ($^\circ\text{C}$ or K)

V: liquid volume (m^3)

V_{molar} : molar volume of a solute ($\text{cm}^3 \text{mol}^{-1}$)

Z: liquid height (m)

Greek letters:

Δt : time interval (s)

μ : dynamic viscosity of the solvent (cP or Pa s)

σ : surface tension (N m^{-1})

τ_G (τ_L): contact time of a gas element (liquid element) at the gas-liquid interface

ρ : density (kg m^{-3})

Superscripts:

eq: at the equilibrium

Subscripts:

exp: from the experiments

G : in the gas phase

i: inlet

L : in the liquid phase

o: outlet

model: from the model

References

- [1] M. Kampa, E. Castanas, Human health effects of air pollution, *Environmental Pollution* 151 (2008) 362-367.
- [2] E.N. Ruddy, L.A. Carroll, Select the best VOC control strategy, *Chemical Engineering Progress* 89 (1993) 28-35.
- [3] F. Khan, I., A. Ghoshal, Kr., Removal of Volatile Organic Compounds from polluted air, *Journal of loss prevention in the process industries* 13 (2000) 527-545.
- [4] S. Revah, J.M. Morgan-Sagastume, Methods of odor and VOC control, *Biotechnology for odor and air pollution control*, Springer 2005, pp. 29-63.
- [5] M. Schlegelmilch, J. Streese, R. Stegmann, Odour management and treatment technologies: an overview, *Waste Management* 25 (2005) 928-939.
- [6] P.-F. Biard, A. Couvert, Overview of mass transfer enhancement factor determination for acidic and basic compounds absorption in water, *Chemical Engineering Journal* 222 (2013) 444-453.
- [7] J.-B. Vilmain, V. Courousse, P.-F. Biard, M. Azizi, A. Couvert, Kinetic study of hydrogen sulfide absorption in aqueous chlorine solution, *Chemical Engineering Research and Design* 92 (2014) 191-204.
- [8] M. Roustan, *Transferts gaz-liquide dans les procédés de traitement des eaux et des effluents gazeux*, Lavoisier, Paris, 2003.
- [9] G. Darracq, A. Couvert, C. Couriol, A. Amrane, P. Le Cloirec, Removal of Hydrophobic Volatile Organic Compounds in an Integrated Process Coupling Absorption and Biodegradation—Selection of an Organic Liquid Phase, *Water, Air, & Soil Pollution* 223 (2012) 4969-4997.
- [10] H. Chen, B. Barna, T. Rogers, D. Shonnard, A screening methodology for improved solvent selection using economic and environmental assessments, *Clean Products and Processes* 3 (2001) 290-302.
- [11] G. Darracq, A. Couvert, C. Couriol, A. Amrane, P. Le Cloirec, Integrated process for hydrophobic VOC treatment—solvent choice, *The Canadian Journal of Chemical Engineering* 88 (2010) 655-660.
- [12] G. Darracq, A. Couvert, C. Couriol, A. Amrane, D. Thomas, E. Dumont, Y. Andres, P. Le Cloirec, Silicone oil: An effective absorbent for the removal of hydrophobic volatile organic compounds, *Journal of Chemical Technology & Biotechnology* 85 (2010) 309-313.
- [13] F. Heymes, P. Manno-Demoustier, F. Charbit, J.L. Fanlo, P. Moulin, A new efficient absorption liquid to treat exhaust air loaded with toluene, *Chemical Engineering Journal* 115 (2006) 225-231.
- [14] S. Guihéneuf, A.S.R. Castillo, L. Paquin, P.-F. Biard, A. Couvert, A. Amrane, Absorption of Hydrophobic Volatile Organic Compounds in Ionic Liquids and Their Biodegradation in Multiphase Systems, *Production of Biofuels and Chemicals with Ionic Liquids*, Springer 2014, pp. 305-337.
- [15] D. Bourgois, D. Thomas, J.L. Fanlo, J. Vanderschuren, Solubilities at high dilution of toluene, ethylbenzene, 1, 2, 4-trimethylbenzene, and hexane in di-2-ethylhexyl, diisooheptyl, and diisononyl phthalates, *Journal of Chemical Engineering Data* 51 (2006) 1212-1215.
- [16] R. Hadjoudj, H. Monnier, C. Roizard, F. Lapique, Absorption of Chlorinated VOCs in High-Boiling Solvents: Determination of Henry's Law Constants and Infinite Dilution Activity Coefficients, *Industrial & Engineering Chemistry Research* 43 (2004) 2238-2246.
- [17] J. Bruneel, C. Walgraeve, K. Van Huffel, H. Van Langenhove, Determination of the gas-to-liquid partitioning coefficients using a new dynamic absorption method (DynAb Method), *Chemical Engineering Journal* (2015).
- [18] M. Guillerm, A. Couvert, A. Amrane, É. Dumont, E. Norrant, N. Lesage, C. Juery, Characterization and selection of PDMS solvents for the absorption and biodegradation of hydrophobic VOCs, *Journal of Chemical Technology and Biotechnology* (2015).
- [19] D. Liu, A. Feilberg, A.M. Nielsen, A.P.S. Adamsen, PTR-MS measurement of partition coefficients of reduced volatile sulfur compounds in liquids from biotrickling filters, *Chemosphere* 90 (2013) 1396-1403.

- [20] F. Wieland, A. Neff, A.N. Gloess, L. Poisson, S. Atlan, D. Larrain, D. Prêtre, I. Blank, C. Yeretian, Temperature dependence of Henry's law constants: An automated, high-throughput gas stripping cell design coupled to PTR-ToF-MS, *International Journal of Mass Spectrometry* (2015).
- [21] D. Bourgois, J. Vanderschuren, D. Thomas, Determination of liquid diffusivities of VOC (paraffins and aromatic hydrocarbons) in phthalates, *Chemical Engineering & Processing: Process Intensification* 47 (2008) 1363-1370.
- [22] R. Hadjoudj, H. Monnier, C. Roizard, F. Lopicque, Measurements of diffusivity of chlorinated VOCs in heavy absorption solvents using a laminar falling film contactor, *Chemical Engineering and Processing: Process Intensification* 47 (2008) 1478-1483.
- [23] E. Dumont, G. Darracq, A. Couvert, C. Couriol, A. Amrane, D. Thomas, Y. Andrès, P. Le Cloirec, Volumetric mass transfer coefficients characterising VOC absorption in water/silicone oil mixtures, *Chemical Engineering Journal* 221 (2013) 308-314.
- [24] R.H. Perry, D.W. Green, *Perry's chemical engineers' handbook*, 7th edition, McGraw-Hill, New-York, 1997.
- [25] S.Y. Lee, Y. Pang Tsui, Succeed at gas/liquid contacting, *Chemical engineering progress* 95 (1999) 23-49.
- [26] J. Staudinger, P.V. Roberts, A critical compilation of Henry's law constant temperature dependence relations for organic compounds in dilute aqueous solutions, *Chemosphere* 44 (2001) 561-576.
- [27] H.J. Benkelberg, S. Hamm, P. Warneck, Henry's law coefficients for aqueous solutions of acetone, acetaldehyde and acetonitrile, and equilibrium constants for the addition compounds of acetone and acetaldehyde with bisulfite, *J Atmos Chem* 20 (1995) 17-34.
- [28] J. Altschuh, R. Brüggemann, H. Santl, G. Eichinger, O.G. Piringger, Henry's law constants for a diverse set of organic chemicals: Experimental determination and comparison of estimation methods, *Chemosphere* 39 (1999) 1871-1887.
- [29] M.D. Vuong, A. Couvert, C. Couriol, A. Amrane, P. Le Cloirec, C. Renner, Determination of the Henry's constant and the mass transfer rate of VOCs in solvents, *Chemical Engineering Journal* 150 (2009) 426-430.
- [30] T.K. Poddar, K.K. Sirkar, Henry's law constant for selected volatile organic compounds in high-boiling oils, *Journal of Chemical & Engineering Data* 41 (1996) 1329-1332.
- [31] B. Xia, S. Majumdar, K. Sirkar, Regenerative oil scrubbing of volatile organic compounds from a gas stream in hollow fiber membrane devices, *Industrial & Engineering Chemistry Research* 38 (1999) 3462-3472.
- [32] E. Dumont, G. Darracq, A. Couvert, C. Couriol, A. Amrane, D. Thomas, Y. Andrès, P. Le Cloirec, Determination of partition coefficients of three volatile organic compounds (dimethylsulphide, dimethylsulphide and toluene) in water/silicone oil mixtures, *Chemical Engineering Journal* 162 (2010) 927-934.
- [33] D. Roizard, F. Lopicque, E. Favre, C. Roizard, Potentials of pervaporation to assist VOCs' recovery by liquid absorption, *Chemical Engineering Science* 64 (2009) 1927-1935.
- [34] R. Higbie, The rate of absorption of a pure gas into still liquid during short periods of exposure, *Transactions of American Institute of Chemical Engineers* 35 (1935) 365-389.
- [35] G. Darracq, *Couplage de l'absorption dans une phase organique et de la biodégradation dans un réacteur multiphasique. Application au traitement de Composés Organiques Volatils hydrophobes*, ENSCR, PhD thesis ENSCR-005, Rennes, 2011.
- [36] F. Heymes, P.M. Demoustier, F. Charbit, J.L. Fanlo, P. Moulin, Hydrodynamics and mass transfer in a packed column: case of toluene absorption with a viscous absorbent, *Chemical Engineering Science* 61 (2006) 5094-5106.
- [37] J. Rejl, V. Linek, T. Moucha, L. Valenz, Methods standardization in the measurement of mass-transfer characteristics in packed absorption columns, *Chemical Engineering Research and Design* 87 (2009) 695-704.

- [38] A. Hoffmann, J. Mackowiak, A. Gorak, M. Haas, J. Loning, T. Runowski, K. Hallenberger, Standardization of mass transfer measurements: a basis for the description of absorption processes, *Chemical Engineering Research and Design* 85 (2007) 40-49.
- [39] I.L. Mostinsky, *A-to-Z Guide to Thermodynamics, Heat & Mass Transfer, and Fluids Engineering* in: <http://www.thermopedia.com/content/696/> (Ed.) Diffusion coefficient, 2011, access date: 15/01/2016.
- [40] T.K. Poddar, S. Majumdar, K.K. Sirkar, Removal of VOCs from air by membrane-based absorption and stripping, *Journal of Membrane Science* 120 (1996) 221-237.
- [41] B. Xia, S. Majumdar, K.K. Sirkar, Regenerative Oil Scrubbing of Volatile Organic Compounds from a Gas Stream in Hollow Fiber Membrane Devices, *Industrial & Engineering Chemistry Research* 38 (1999) 3462-3472.

ACCEPTED MANUSCRIPT

Appendix 1. Calculation of the VOC diffusion coefficients in DEHA and PDMS

Table A.1: Calculation of the liquid diffusion coefficients ($10^{-10} \text{ m}^2 \text{ s}^{-1}$) by different correlations at 293 K (PDMS case).

	Wilke-Chang ^a	Scheibel ^a	Tyn and Calus ^b	Hayduk and Minhas ^b	Siddiqi and Lucas ^b
Toluene	1.40	1.98	122	0.80	0.84
	Experimental values : 7.63 at 298 K ^c , 2.52 ^d , 0.57 to 2 ^e				
Dichloromethane	1.99	3.51	160	1.03	1.09
Propanol	1.74	2.82	148	0.95	0.98
Acetone	1.80	2.99	150	0.97	1.01

^a [39], ^b [22], ^c [40], ^d [41], ^e [35]

Table A.2: Calculation of the diffusion coefficients ($10^{-10} \text{ m}^2 \text{ s}^{-1}$) by different correlations at 293 K (DEHA case).

	Wilke-Chang ^a	Scheibel ^a	Tyn and Calus ^b	Hayduk and Minhas ^b	Siddiqi and Lucas ^b
Toluene	1.90	2.23	72.1	1.70	1.68
Dichloromethane	2.71	3.78	94.1	2.19	2.18
Propanol	2.37	3.09	87.3	2.02	1.97
Acetone	2.45	3.26	88.3	2.05	2.03

^a [39], ^b [22]

All the physico-chemical properties required for the diffusion coefficient calculation are summarized in Table A3.

Table A.3 Physicochemical properties of the VOC and solvents required for liquid diffusion coefficients calculation at 293 K.

	Toluene	Acetone	Isopropanol	Dichloromethane	DEHA	PDMS
ρ at T_b (kg m^{-3})	779	749	731	1290		
V_{molar} ($\text{cm}^3 \text{ mol}^{-1}$)	118.5	77.5	82.2	65.8	402	3.3×10^3
σ (mN m^{-1})	28.5	25.2	23.0	26.5	31	20.8
$P\alpha$ ($\text{g}^{1/4} \text{ cm}^3 \text{ mol}^{-1} \text{ s}^{-1/2}$)	274	174	180	149	950	7.1×10^3

Appendix 2. Mathematical treatment of the mass-transfer differential equations system

Eqs. 5 and 11 leads to:

$$\Rightarrow \frac{V}{\Delta t} (C_L^{t+\Delta t} - C_L^t) = \frac{K_L a^\circ V}{H_d} \frac{C_{G,j} - \bar{C}_{G,o}}{\ln \frac{C_{G,j} - H_d \bar{C}_L}{C_{G,o} - H_d \bar{C}_L}} \quad \text{Eq. 25.}$$

The average gas outlet concentration $\bar{C}_{G,o}$ can be deduced from Eq. 26 with the help of Eqs Eqs. 5 and 12:

$$\bar{C}_{G,o} = C_{G,j} - \frac{V}{F_G} \frac{2(\bar{C}_L - C_L^t)}{\Delta t} \quad \text{Eq. 26.}$$

Then, Eqs 12 and 25 leads to:

$$\Rightarrow \frac{2V(\bar{C}_L - C_L^t)}{\Delta t} = \frac{\frac{2V^2 K_L a^\circ (\bar{C}_L - C_L^t)}{H_d F_G \Delta t}}{\ln \frac{C_{G,j} - H_d \bar{C}_L}{C_{G,j} - \frac{V}{F_G} \frac{2(\bar{C}_L - C_L^t)}{\Delta t} - H_d \bar{C}_L}} \quad \text{Eq. 27.}$$

$$\Rightarrow \ln \frac{\frac{C_{G,j} - \bar{C}_L}{H_d}}{\frac{C_{G,j} - \frac{V}{H_d F_G} \frac{2(\bar{C}_L - C_L^t)}{t^{j+1} - t^j} - \bar{C}_L}{H_d}} = \frac{VK_L a^\circ}{H_d F_G} \quad \text{Eq. 28.}$$

$$\Rightarrow \frac{\frac{C_{G,j} - \bar{C}_L}{H_d}}{\frac{C_{G,j} - 2A(\bar{C}_L - C_L^t) - \bar{C}_L}{H_d}} = \exp(AK_L a^\circ \Delta t) = \exp(B) \quad \text{Eq. 29.}$$

$$\text{With } A = \frac{V}{H_d F_G \Delta t} \text{ and } B = AK_L a^\circ \Delta t = \frac{K_L a^\circ V}{H_d F_G}$$

Then:

$$\bar{C}_L = \frac{C_{G,i}(1-\exp(B)) - 2AC_L^t \exp(B)}{H_d(1-\exp(B)(1+2A))} \quad \text{Eq. 30.}$$

Therefore, the liquid concentration and the gas concentration at $t + \Delta t$ can be calculated through respectively Eq. 31 (deduced from Eq. 12) and Eq. 32 (deduced from Eqs 4 and 26):

$$C_L^{t+\Delta t} = 2 \frac{C_{G,i}(1-\exp(B)) - 2AC_L^t \exp(B)}{H_d(1-\exp(B)(1+2A))} - C_L^t \quad \text{Eq. 31.}$$

$$C_{G,o}^{t+\Delta t} = 2\bar{C}_{G,o} - C_{G,o}^t = 2 \left(C_{G,i} - \frac{V}{F_G(t^{j+1} - t^j)} (C_L^{t+\Delta t} - C_L^t) \right) - C_{G,o}^t \quad \text{Eq. 32.}$$

ACCEPTED MANUSCRIPT

- Heavy solvents (DEHA and PDMS) and water were assessed for the absorption of four VOC
- A simple and timesaving experimental procedure was developed
- Partition and mass-transfer coefficients were deduced from the experiments
- The two organic solvents tested, especially DEHA, exhibited rather good affinity with all VOC
- The liquid-film coefficient was 500% higher in PDMS and 30% higher in DEHA than in water

ACCEPTED MANUSCRIPT